Investigations on Corrosion Behaviour of AA 8011-ZrB_2 in Situ Metal Matrix Composites

B. M. Muthamizh Selvan and V. Anandakrishnan

Abstract The composite system of AA 8011-ZrB_2 (0, 4 and 8 wt%) was synthesized by using economical and efficient fabrication method of in situ stir casting technique and the corrosion behaviour was investigated. The fabricated samples were exposed to X-ray diffraction and scanning electron microscope to confirm the existence of ZrB_2 and for the study of the morphology of ZrB_2 particles in aluminium composites, respectively, and also the ZrB_2 particles were clearly located by using energy dispersive spectroscopy. The corrosion behaviour of the synthesized composite system was investigated in NaCl solution and the inclusion of in situ formed ZrB_2 in AA 8011 improved the corrosion resistance, it was evidently proved through scanning electron microscope images.

Keywords Aluminium · Metal matrix composites · In situ stir casting · Corrosion behaviour · Potentiodynamic polarization

1 Introduction

Aluminium matrix composites lead the race among the metal matrix composites in current research and utilization due to its low cost, ease of production and other attractive properties such as high specific strength, high specific stiffness, the low thermal coefficient of expansion, improved tribological and corrosion resistance. Due to such incredible properties, aluminium matrix composites have attracted great scientific attention as the promising candidate which is used in wide range of applications includes recreation, sports, packaging, precision instruments, biotechnology, automotive, aerospace, military, nuclear, electronic thermal management and marine industries [1–4]. In the fabrication of corrosive and cryogenic environment application products like Arctic chemical processing equipment, Moss- and SPB-type tanks

B. M. Muthamizh Selvan (✉) · V. Anandakrishnan
Department of Production Engineering, National Institute of Technology, Tiruchirappalli 620015, India
e-mail: muthamizh.bm@gmail.com

S. S. Hiremath et al. (eds.), *Advances in Manufacturing Technology*, Lecture Notes in Mechanical Engineering,
https://doi.org/10.1007/978-981-13-6374-0_39

(LNG carrier insulation systems), subsea pipelines, pressure vessels and drill pipes (offshore structures) aluminium metal matrix composite play a vital role [5]. Aluminium composites are fabricated through various techniques such as centrifugal casting, squeeze casting, powder metallurgy, stir casting (ex situ) and reactive processing (in situ) [6]. Fabrication of the aluminium metal matrix composites through in situ route provides several advantages such as ease of production, economical, grain refinement, thermodynamic stability, uniform distribution of reinforcements, the excellent bonding strength between matrix and reinforcement. ZrB_2 owns fabulous properties such as high melting temperature, good thermal conductivity, excellent mechanical properties, oxidation resistance, elastic modulus and resistance to chemical attack [7]. In situ formed ZrB_2 was fabricated in aluminium alloy through reaction of K_2ZrF_6 and KBF_4 with molten aluminium alloy. The fine and homogeneous distribution of ZrB_2 particles in aluminium alloy was confirmed through micro-structural studies and due to the incorporation of the in situ ZrB_2 particles, the mechanical properties of the aluminium alloy were amplified [8]. The AA 2618 matrix was reinforced with AlN, Si_3N_4, and ZrB_2 (0, 2, 4, 6, and 8), and the ZrB_2 has been synthesized in AA 2618 matrix through in situ stir casting technique by mixing K_2ZrF_6 and KBF_4 in molten AA 2618 alloy. Increase in the percentage of ZrB_2 enhanced the corrosion resistance in aluminium composite [9].

From the above literature survey, it is clear that the aluminium matrix composites are used in real-time application which requires corrosion resistance and the addition of reinforcements in aluminium matrix had cemented the route for the enrichment of corrosion resistance. The in situ stir casting technique offers the fine and homogeneous distribution of reinforcements in aluminium matrix economical approach. In this paper, AA 8011-ZrB_2 (0, 4 and 8 wt%) is synthesized through in situ stir casting technique and the synthesized materials are involved in X-ray diffraction and scanning electron microscope (SEM) to study the presence and distribution of the ZrB_2 particles. Corrosion behaviour of the samples was investigated through the potentiodynamic polarization technique.

2 Experimental Procedure

2.1 Fabrication of Materials

AA 8011 was tested to confirm the material compositions as per the ASTM-B-209 M, given in Table 1. The composite system of AA 8011-ZrB_2 (0, 4 and 8 wt%) was fabricated by using an in situ stir casting technique. AA 8011 rods were heated in the graphite crucible at the temperature of 860°. Stoichiometrically, calculated halide salts (K_2ZrF_6 and KBF_4) as given in Table 2 were added to the molten form of aluminium which was preheated at the temperature of 250 °C for the removal of moisture. Stirring was carried out for every 5 min by using graphite rod to distribute the halide salts homogeneously and the time allowed for completion of the reaction is

Table 1 Chemical composition of AA 8011 alloy (%)

Si	Fe	Cu	Mn	Mg	Cr	Zn	Ti	Al
0.6	0.7	0.25	0.15	0.9	0.2	0.25	0.15	Remaining

Table 2 Quantity of halide salts added for obtaining various compositions of materials

Salts in gm	AA 8011-0 wt% ZrB_2	AA 8011-4 wt% ZrB_2	AA 8011-8 wt% ZrB_2
K_2ZrF_6	0	100.45	200.91
KBF_4	0	89.25	178.51

30 min. During these processes, exothermic reactions take place between the halide salts and aluminium matrix is shown (1), (2) and (3)

$$3K_2ZrF_6 + 13Al \rightarrow 3Al_3Zr + 2K_3AlF_6 + 2Al \quad (1)$$

$$6KBF_4 + 9Al \rightarrow 3AlB_2 + 2K_3AlF_6 + 4AlF_3 \quad (2)$$

$$AlB_2 + Al_3Zr \rightarrow ZrB_2 + 4Al \quad (3)$$

After the completion of the in situ reaction, elements other than ZrB_2 were evaporated or removed as slag and the process parameters were decided through literature reviews of [8].

2.2 Corrosion Study

The electrochemical corrosion behaviour of AA 8011-ZrB_2 (0, 4 and 8 wt%) was investigated by potentiodynamic polarization (PDP) technique in 3 wt% of sodium chloride solution using IVIUM electrochemical workstation with the three electrode system. The calomel electrode as reference, graphite as counter electrode and the sample under test acted as the working electrode. The PDP curves were obtained in the potential range of −500 to +500 mV with reference to OCP with the scan rate of 1 mV/s. The Tafel extrapolation was used to calculate the E-Corr and i-Corr values from the PDP curves which is helpful to evaluate the corrosion resistance of the synthesized aluminium materials.

3 Results and Discussion

3.1 X-Ray Diffraction (XRD) Analysis

Figure 1 shows the X-ray diffractogram of AA 8011-0 wt% ZrB_2, AA 8011-4 wt% ZrB_2 and AA 8011-8 wt% ZrB_2 which were performed in RINGKU X-ray diffraction machine. The peak intensities of (002), (022), (113) aluminium rise with the increasing addition of ZrB_2. This denotes that ZrB_2 acts as a pinning particle to arrest the grain growth of aluminium which leads to smaller crystallite size. The ZrB_2 appears at the vicinity of 2θ positions (24.99), (32.39), (41.45), (73.90) which confirms the presence of reinforced ZrB_2.

3.2 Micro-Structural Analysis

The microstructure of the fabricated composite system was studied through HITACHI SU 3000 SEM machine and the SEM images are shown in Fig. 2a–e. Figure 2a clearly indicates the absence of ZrB_2 particles along the grain boundaries, but the presence of ZrB_2 along the grain boundaries of the aluminium matrix is observed in Fig. 2b–c some particles were observed along the grain boundaries of AA 8011-4 wt% ZrB_2 and AA 8011-8 wt% ZrB_2. The magnified SEM image of the particles of Fig. 2c was

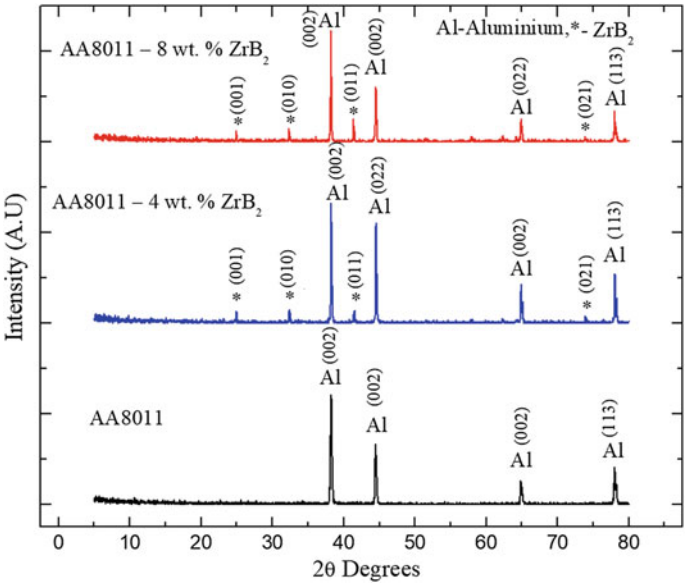

Fig. 1 X-Ray diffraction results of as casted AA-8011 and composites

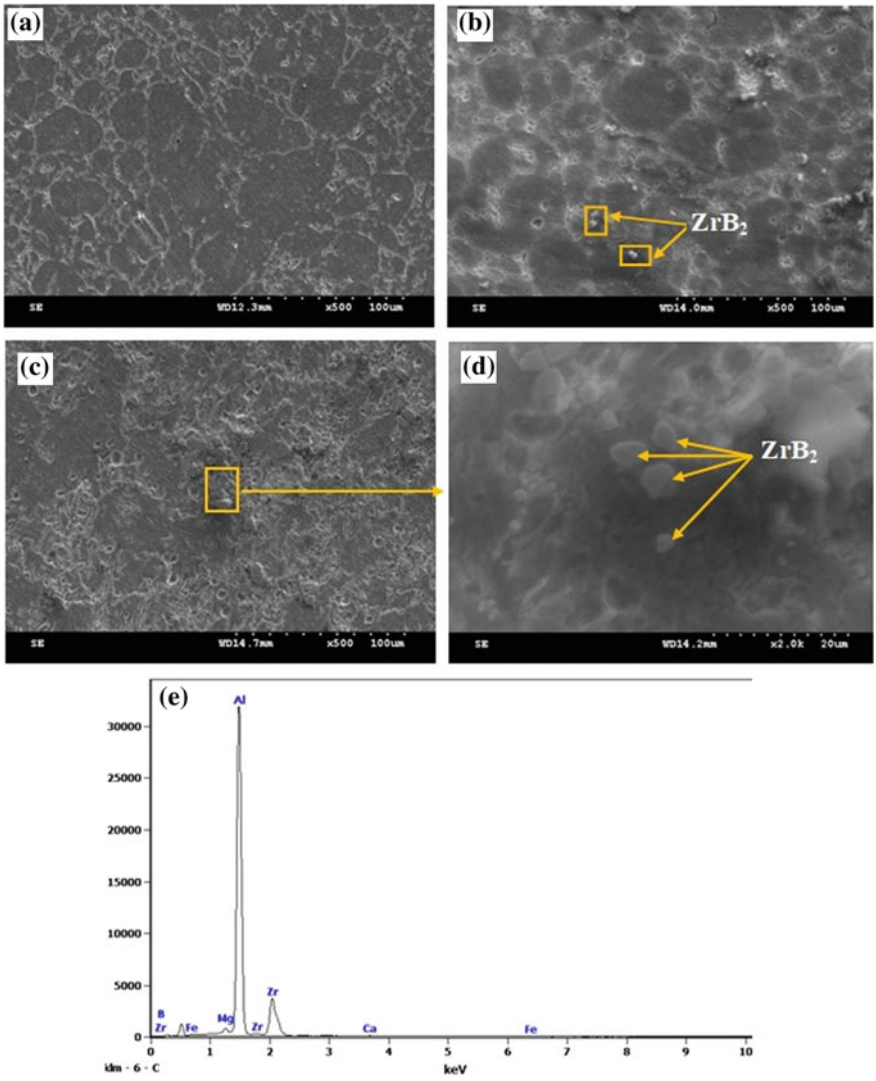

Fig. 2 SEM images of **a** AA8011, **b** AA8011- 4 wt% ZrB_2, **c** AA8011-8 wt% ZrB_2, **d** magnified SEM image of ZrB_2, **e** energy dispersive spectroscopy of Fig. 2d

captured and the magnified view is shown in Fig. 2d which evidently proved as ZrB_2 particles by the spectrum (Fig. 2e) and it shows the peaks of Al, Zr and B which were obtained from energy dispersive can be observed clearly and their percentages are given in Table 3. The distribution of the ZrB_2 is uniform and homogeneous along the grain boundaries of aluminium matrix and both AA 8011-4 wt% ZrB_2 and AA 8011-8 wt% ZrB_2 which is evidently visible Fig. 2b–c. The uniform distribution of the ceramic particles in aluminium matrix is significantly influenced by the density

Table 3 Elemental analysis of energy dispersive spectroscopy

Element	Weight (%)	Atomic (%)
Al K	73.85	90.09
Zr L	25.67	9.26
Mg K	0.48	0.64
Total	100.00	100.00

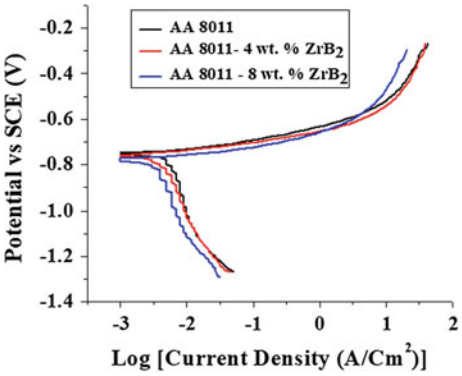

Fig. 3 Potentiodynamic polarization curves of the samples, **a** AA8011-0 wt% ZrB_2, **b** AA8011-4 wt% ZrB_2 and **c** AA8011-8 wt% ZrB_2

difference between the ceramic particles and aluminium particles. When the density difference between the ceramic particle and aluminium matrix is greater than 2 g/cm^3 during solidification, this makes ceramic particles to sink easily in molten aluminium and to be suspended for a long time. The density difference between the molten AA 8011 matrix and in situ formed ZrB_2 is more than 2 g/cm^3 which paves the way for the uniform distribution of ZrB_2 along the grain boundaries. Also, the wetting property between the ceramic particles and molten aluminium matrix arrests the movement of ZrB_2 particles which leading to the long-time suspension of ZrB_2 particles in molten aluminium matrix during solidification for better distribution of ceramic particles [10].

3.3 Electrochemical Studies

3.3.1 Potentiodynamic Polarization

The corrosion behaviour was studied by potentiodynamic polarization (PDP) test conducted by exposing the surface area of 0.5 mm^2 in sodium chloride solution. The PDP curves for aluminium samples are shown in Fig. 3a–c it clearly says that the curve is shifting right side to left side with the addition in the percentage of

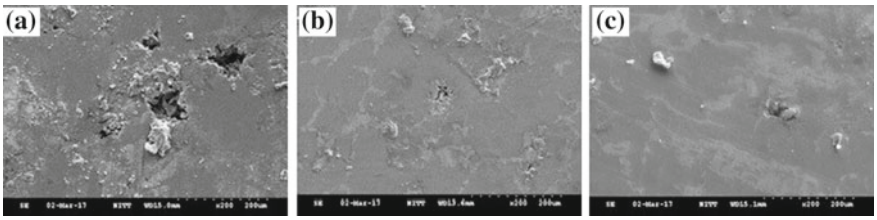

Fig. 4 SEM image of corroded surfaces of AA8011 matrix composites with ZrB_2 reinforcement, **a** 0 wt%, **b** 4 wt%, and **c** 8 wt%

Table 4 Experimental results obtained from potentiodynamic polarization curves

Name of the material	E-Corr (V)	i-Corr (A)	Corrosion rate (mm/year)
AA8011-0 wt% ZrB_2	−0.7505	2.15×10^{-7}	1.1560
AA8011-4 wt% ZrB_2	−0.7594	1.73×10^{-7}	0.9304
AA8011-8 wt% ZrB_2	−0.7746	1.61×10^{-7}	0.8672

reinforcement and this demonstrates the decrement in i-corr value. The corrosion current density or i-Corr values reveal the flow of current in open circuit potential as a result of the reduction reaction. The i-Corr values are inversely proportional to the corrosion resistance. Corrosion potential (E-Corr) values demonstrate the ionization tendency of a material in NaCl solution [11, 12]. The E-Corr and i-Corr values are tabulated in Table 4 which undoubtedly establishes that the increase in the percentage of ZrB_2 is inversely proportional to the i-corr value. Also, the corrosion rate in AA 8011 alloy is reduced from 1.156 to 0.8672 by reinforcing it with the ceramic of ZrB_2 is evident that addition of ZrB_2 will enhance the corrosion resistance [9]. Because the ZrB2 possess the excellent chemical inertness which provides excellent resistance to chemical attack, oxidation and corrosion [8].

Figure 1 confirms the presence of ZrB_2 and the SEM images that were captured as shown in Fig. 2b–c that the reinforcement is unvaryingly distributed along the grain of AA 8011 alloy which is essential for improving corrosion resistance. The SEM images that captured in the corrosion surfaces are shown in Fig. 4a–c supports the previous statement depicts that addition of ZrB_2 in aluminium alloy has clearly arrested the corrosion. Figure 4a displays that AA 8011 had been severely corroded in the NaCl solution but Fig. 4b–c reveals that AA 8011-4 wt% ZrB_2 and AA 8011-8 wt% ZrB_2 had shown resistance to corrosion in NaCl solution.

4 Conclusion

1. The AA 8011-ZrB_2 (0, 4 and 8 wt%) was successfully fabricated through in situ stir casting technique.

2. Corrosion behaviour of fabricated aluminium samples AA 8011-ZrB_2 (0, 4 and 8 wt%) was investigated in sodium chloride environment and evaluated by using potentiodynamic polarization technique with reference to open circuit potential by using three electrochemical cell system.
3. The presence of ZrB_2 was confirmed by XRD analysis and energy dispersive spectroscopy.
4. The homogeneous distribution of ZrB_2 along the grain boundaries of aluminium was confirmed through SEM images.
5. The corrosion resistance was improved in AA 8011 by the inclusion of ZrB_2 and the AA8011-8 wt% ZrB_2 exhibits the superiority in corrosion resistance.

References

1. Oladijo OP, Bodunrin MO, Sobiyi K, Maledi NB, Alaneme KK (2016) Investigating the self-healing behaviour of under-aged and 60Sn–40Pb alloy reinforced aluminium hybrid composites. Thin Solid Films 620:201–205
2. Kaushik NC, Rao RN (2016) Effect of grit size on two body abrasive wear of Al 6082 hybrid composites produced by stir casting method. Tribol Int 102:52–60
3. Natarajan N, Vijayarangan S, Rajendran I (2006) Wear behaviour of A356/25SiCp aluminium matrix composites sliding against automobile friction material. Wear 261(7–8):812–822
4. Kumar S, Panwar RS, Pandey OP (2013) Effect of dual reinforced ceramic particles on high temperature tribological properties of aluminum composites. Ceram Int 39(6):6333–6342
5. Kumar PSR, Smart DR, Alexis SJ (2017) Corrosion behaviour of aluminium metal matrix reinforced with multi-wall carbon nanotube. J Asian Ceram Soc 5(1):71–75
6. Baskaran S, Anandakrishnan V, Duraiselvam M (2014) Investigations on dry sliding wear behavior of in situ casted AA7075–TiC metal matrix composites by using Taguchi technique. Mater Des 60:184–192
7. Gaurav G, Anitha M (2015) Effect of ZrB_2 particles on the microstructure and mechanical properties of hybrid (ZrB_2+Al_3Zr)/AA5052 insitucomposites. J Alloy Compd 649:174–183
8. Kumar N, Gautam RK, Mohan S (2015) In-situ development of ZrB_2 particles and their effect on microstructure and mechanical properties of AA5052 metal-matrix composites. Mater Des 80:129–136
9. Kumar NM, Kumaran SS, Kumaraswamidhas LA (2015) An investigation of mechanical properties and corrosion resistance of Al2618 alloy reinforced with Si_3N_4, AlN and ZrB_2 composites. J Alloy Compd 652:244–249
10. Dinaharan I, Murugan N, Parameswaran S (2011) Influence of in situ formed ZrB_2 particles on microstructure and mechanical properties of AA6061 metal matrix composites. Mater Sci Eng, A 528(18):5733–5740
11. Sathiya P, Ramesh T (2017) Experimental investigation and characterization of laser welded NiTinol shape memory alloys. J Manufact Process 25:253–261
12. Kannan TDB, Ramesh T, Sathiya P (2016) A review of similar and dissimilar micro-joining of nitinol. JOM 68(4):1227–1245